Proteasome Inhibitors

International Edition: DOI: 10.1002/anie.201502931
German Edition: DOI: 10.1002/ange.201502931

A Minimal β-Lactone Fragment for Selective β5c or β5i Proteasome Inhibitors**

Michael Groll, Vadim S. Korotkov, Eva M. Huber, Armin de Meijere, and Antje Ludwig**

Abstract: *Broad-spectrum proteasome inhibitors are applied as anticancer drugs, whereas selective blockage of the immunoproteasome represents a promising therapeutic rationale for autoimmune diseases. We here aimed at identifying minimal structural elements that confer β5c or β5i selectivity on proteasome inhibitors. Based on the natural product belactosin C, we synthesized two β-lactones featuring a dimethoxybenzyl moiety and either a methylpropyl (pseudo-isoleucin) or an isopropyl (pseudo-valine) P1 side chain. Although the two compounds differ only by one methyl group, the isoleucine analogue is six times more potent for β5i (IC_{50} = 14 nM) than the valine counterpart. Cell culture experiments demonstrate the cell-permeability of the compounds and X-ray crystallography data highlight them as minimal fragments that occupy primed and non-primed pockets of the active sites of the proteasome. Together, these results qualify β-lactones as a promising lead-structure motif for potent nonpeptidic proteasome inhibitors with diverse pharmaceutical applications.*

The eukaryotic 20S proteasome (core particle, CP), a multicatalytic protease of 720 kDa that is responsible for non-lysosomal protein degradation, is a key player in many cellular processes, including cell cycle progression and the immune response.[1] Whereas yeast harbors one 20S proteasome (yCP), there are three individual CP types in vertebrates and they differ only in the composition of their proteolytically active subunits: the constitutive proteasome (cCP), the immunoproteasome (iCP), and the thymoproteasome (tCP).[2] Protein breakdown occurs in the central lumen of each of the CPs and peptide bond cleavage by all of the active sites follows a universal principle. It is thus the unique chemical nature of the specificity (S) pockets that gives rise to distinct substrate preferences through interaction with the side chains of the ligand (P sites).[3] As a rule, the cleavage specificities of the three proteasomal active sites are assigned by using chromogenic screening substrates and relate to the preferred P1 amino acid. In this way, subunit β1 (caspase-like; C-L) was determined to cleave after acidic residues, β2 (trypsin-like; T-L) after basic residues, and β5 (chymotrypsin-like; ChT-L) after non-polar residues.[4]

Increased expression levels of the iCP or its active subunits β1i, β2i, and β5i have recently been associated with the development and progression of neurodegenerative diseases,[5] autoimmune disorders,[6] and certain types of cancers.[7] ONX 0914, a β5i-selective peptidic α′,β′-epoxyketone inhibitor, has been shown to suppress autoreactive immune responses in mouse models of rheumatoid arthritis, lupus, and experimental encephalomyelitis by preventing the production of interleukins and the release of interferon-γ.[8] Crystallographic data for the murine cCP and iCP identified the differently sized S1 pockets in β5c and β5i, formed by unique orientations of Met45, as the major determinant of the enhanced affinity of ONX 0914 for β5i. Based on the observation that ligands dock via their P1 residue to the active site, compounds with large P1 residues were supposed to favour β5i, whereas small P1 side chains were suggested to be more appropriate for β5c.[9]

Successive drug design efforts have succeeded in improving existing β5i inhibitors by exchanging their P1-phenylalanine moiety for a cyclohexyl residue.[10] However, all of these currently available proteasome inhibitors feature a peptide-based backbone that only targets the non-primed sites of the substrate binding channel shaped by the subunits β5 and β6. Considering that subunit β6 is unchanged between cCP and iCP, pronounced interactions of the ligand with β6 are supposed to hamper β5i selectivity. We therefore aimed at developing small nonpeptidic proteasome inhibitors that target both the primed and non-primed sites solely of subunit β5. As a scaffold, we used the bisbenzyl-protected homobelactosin C (**1**; Figure 1 A), a derivative of the natural product β-lactone belactosin C from *Streptomyces* sp. UCK14.[11] Unlike the family of β-lactone-γ-lactam inhibitors, including the microbial metabolite omuralide (clasto-lactacystin, **2**; Figure 1 A),[4a,12] crystallographic data demonstrated that **1** only binds to β5, even at concentrations as high as 20 mM.[13] Notably and in contrast to **2**, belactosin C and its derivatives occupy both the S1 specificity pocket and the previously neglected primed substrate binding channel, including the adjacent subunit β4.[13,14] In order to address

[*] Prof. Dr. M. Groll, Dr. V. S. Korotkov, Dr. E. M. Huber
Center for Integrated Protein Science at the Department Chemie
Technische Universität München
Lichtenbergstrasse 4, 85748 Garching (Germany)
E-mail: michael.groll@tum.de
Dr. A. Ludwig
Charité Universitätsmedizin Berlin CCM
Medizinische Klinik für Kardiologie und Angiologie
Charitéplatz 1, 10117 Berlin (Germany)
E-mail: antje.ludwig@charite.de
Prof. Dr. A. de Meijere
Institut für Organische und Biomolekulare Chemie der
Georg-August-Universität Göttingen
Tammannstrasse 2, 37077 Göttingen (Germany)

[**] This work was supported by the Deutsche Forschungsgemeinschaft (DFG, grant GR1861/10-1 to M.G.). A. König is acknowledged for excellent technical support. We are grateful to the staff of the beamline BW6, DESY, Hamburg (Germany).

Supporting information for this article is available on the WWW under http://dx.doi.org/10.1002/anie.201502931.

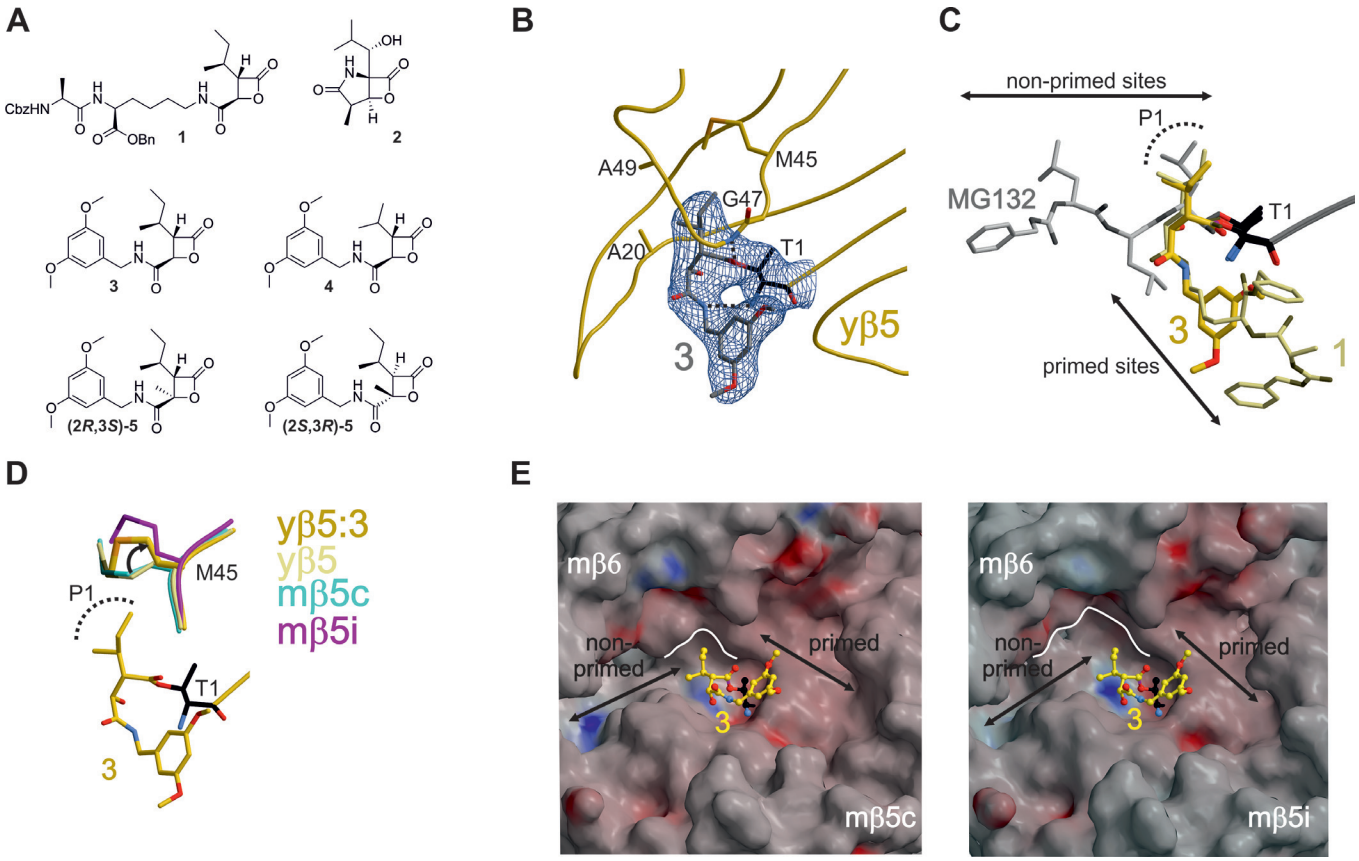

Figure 1. A) Structures of bisbenzylated homobelactosin C (**1**), omuralide (**2**), and the analyzed β-lactones **3**–**5**. B) Crystal structure of yCP:**3** at the yβ5 active site (PDB ID 4Z1L). The $2F_O-F_C$ electron density map (blue mesh, contoured at 1.0 σ) is shown for **3** and the active site Thr1; dotted lines mark hydrogen bonds to the oxyanion hole Gly47NH and to Thr1NH_2. Met45 forms the bottom of the S1 pocket and determines the affinity and specificity of inhibitor binding. C) The superposition of **1**,[13] **3**, and MG132[16] at yβ5 shows that the peptidic compound MG132 solely binds to the non-primed sites S1–S3, whereas homobelactosin C (**1**) and its derivative (**3**) occupy the S1 pocket (the P1 site of the ligand is marked by a dotted half circle) and the primed pockets. D) The superposition of yeast and mouse β5 subunits reveals the distinct conformations of Met45.[9] The black arrow marks the reorientation of Met45 upon binding of **3** to yβ5. The Ile-like P1 site of **3** (marked by a dotted half circle) undergoes hydrophobic interactions with all Met45 conformations and hence does not discriminate between β5c and β5i. E) Connolly surface representations of mouse β5c and β5i active sites with **3** modelled by the superposition of yβ5:**3**. Positive and negative electrostatic surface potentials are contoured from $-30\ kTe^{-1}$ (red) to $30\ kTe^{-1}$ (blue). For clarity, residues 47 and 48 of β5 have been removed. The S1 pockets are indicted by a white line to illustrate their different sizes in β5c and β5i (see also Figure S1C). It should be noted that binding of the P1-Ile side chain to β5c requires the reorientation of Met45 as in yβ5 in panel D to avoid clashing.

solely subunit β5 and to identify structural elements that discriminate between β5c and β5i, we investigated a series of belactosin C derivatives.[14,15] In the course of these investigations, we found a minimal scaffold that is suitable for high-affinity binding to β5. These fragments feature a *N*-(3,5-dimethoxybenzyl)aminocarbonyl side chain at the C2 position of either a (3*S*)-((1*S*)-methylpropyl)- (isoleucine mimetic **3**; Figure 1 A) or a (3*S*)-(isopropyl)-4-oxooxetane-(2*R*)-carboxamide (valine mimetic **4**; Figure 1 A) moiety.[15]

X-ray crystallographic analysis of **3** in complex with the yCP was performed according to our standard protocols[17] and yielded data to 3.0 Å resolution with an R_{free} of 22.9 % (see Table S1 in the Supporting Information). The electron density map displayed the inhibitor covalently bound to the N-terminal Thr1O^{γ} of all of the active sites owing to the high ligand concentrations used for crystal soaking (Figure 1 B and Figure S1A in the Supporting Information). Interestingly, superposition of **3** bound to yβ1, yβ2, and yβ5 shows that the ligand adopts a uniform orientation in each substrate binding channel (Figure S1B). The isoleucine P1 side chain protrudes into the S1 specificity pocket and causes a 1 Å shift of Met45, whereas the C2-OH group of the ligand, generated through nucleophilic attack of Thr1O^{γ} on the β-lactone ring, forms a strong hydrogen bond to the carbonyl oxygen of residue 19 (2.7 Å), as observed for homobelactosin C.[13,18] The 3,5-dimethoxybenzyl group points towards the primed substrate binding channel and is only stabilized by hydrophobic interactions with C^{α} and C^{β} of Ser129, a strictly conserved residue involved in catalysis.[13] In conclusion, the crystallographic investigations of **3** provide first insight into the primed substrate binding channels of the C-L and T-L active sites. The common binding mode of **3** with all three active sites implies that the subunit selectivity of compounds mainly depends on their interactions with the primed and non-primed specificity pockets of the individual binding clefts. The described minimal scaffold required to orient ligands to the

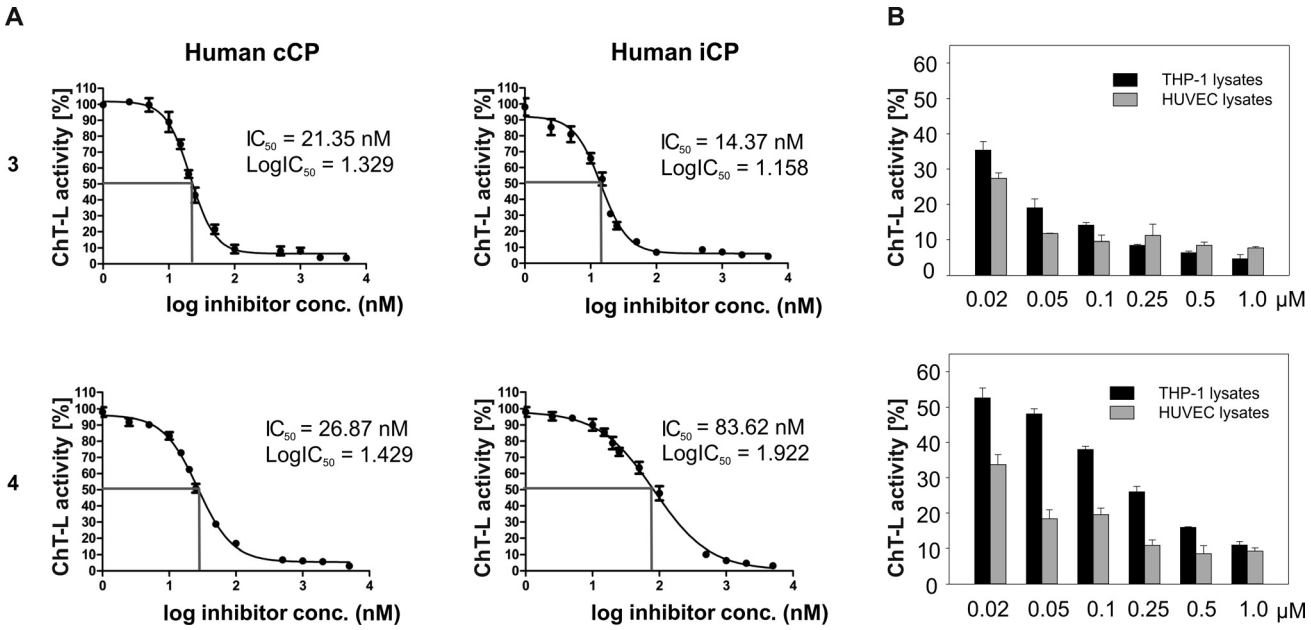

Figure 2. A) Dose–response curves for **3**- and **4**-mediated inhibition of the ChT-L activities of human cCP and iCP. Experiments were performed in triplicate and normalized to a DMSO-treated control. B) Inhibition profiles of **3** and **4** in lysates of HUVEC (cCP) and monocytic THP-1 (predominantly iCP) cells. Values are given as the mean percentage of residual activity ± standard error of the mean (SEM).

primed site of all active β subunits is now amenable to future combinatorial chemistry to create selective compounds for individual active sites.

Next, we characterized the belactosin derivatives **3** and **4**, which only differ in a single P1-methyl group, for their inhibitory potency towards human cCP and iCP. Indeed, **3** and **4** dose-dependently block the ChT-L activity of β5c and β5i owing to their apolar moieties (Figure 2A). Although both compounds feature no P2, P3, or P4 sites, they are highly effective. Interestingly, the half maximal inhibitory concentration (IC_{50}) values for **3** are quite similar for β5c (21.35 nM) and β5i (14.37 nM), whereas **4** turned out to be more selective for β5c (26.87 nM) than for β5i (83.62 nM). Hence, the single P1-methyl group that distinguishes **3** from **4** is decisive in terms of subunit selectivity. Additionally we performed inhibition assays with lysates from human umbilical vein endothelial cells (HUVEC, which contain predominantly cCP) and THP-1 cells (a human monocytic leukemia cell line containing predominantly iCP). Increasing concentrations of **3** blocked ChT-L activity in lysates of both cell types to a similar degree, while **4** was more potent in HUVEC lysates (Figure 2B). Although the tested hydrophobic P1 residues are accepted by both β5c and β5i, the herein presented results prove that the ChT-L activity of β5i demands more bulky amino acids compared to β5c and disfavors smaller ones like Val.[9] The peculiar conformation of Met45 in subunit β5i enlarges the S1 pocket and cannot properly stabilize the smaller P1-Val side chain of **4** by van der Waals contacts (Figure 1D,E).

In addition, we investigated the effect of **3** and **4** on proteasome activity in living mammalian cells. HeLa cells were treated for 4 h with varying concentrations of **3**, **4** and the standard proteasome inhibitor Z-Leu-Leu-Leu-al (MG132); DMSO was used as the solvent control (see the Supporting Information). In vitro activity assays in cell lysates revealed that **3** and **4** dose-dependently inhibit proteasome-mediated protein degradation and predominantly affect ChT-L activity (Figure 3A). As expected, the CP inhibition results in a breakdown in overall proteasomal function, thereby causing an accumulation of a destabilized GFP reporter in ear fibroblasts of the $Ubiquitin^{G76V}$-GFP1-mouse (Figure 3B, upper panel) and an increase in polyubiquitylated proteins (Figure 3B, lower panel). We quantified the cytotoxicity by treating HeLa cells with 500 nM and 1 μM of **3** and **4** in an MTT (3-[4,5-dimethylthiazol-2-yl]-2,5-diphenyl tetrazolium bromide) cell proliferation assay for 24 h. Remarkably, cell viability was twice as high upon the application of **3** and **4** compared to the standard proteasome inhibitor MG132 (Figure 3C), a significant and important feature for the future development of selective CP-type drugs for non-cancer applications such as inflammation or autoimmune diseases. Moreover, we performed flow cytometry cell cycle analysis with HeLa cells incubated with both compounds at a concentration of 500 nM for 24 h (see Supporting Information). Distinct sub-G1 peaks (corresponding to apoptotic cells) were observed after treatment with **3** (8.91 ± 0.44 % of all cells), **4** (10.03 ± 1.08 %), and MG132 (19.68 ± 2.04 %). The increased numbers of cells in the G2/M phase demonstrate that both compounds induce cell cycle arrest in HeLa cells (control: 12.31 ± 0.84 %, **3**: 23.78 ± 0.49 % and **4**: 23.36 ± 2.62 % of all non-apoptotic cells), albeit to a much less pronounced degree than MG132 (40.36 ± 2.87 %). In addition to **3** and **4**, we tested the β-lactones (2*R*, 3*S*)-**5** and (2*S*, 3*R*)-**5**[14,15] in our biological assays. Both compounds feature an additional methyl group at the C2 position of compound **3**, which was derived from the natural product Salinosporamide A (marizomib),[19] a second generation proteasome inhibitor currently being evaluated in clinical trials. Surprisingly, the

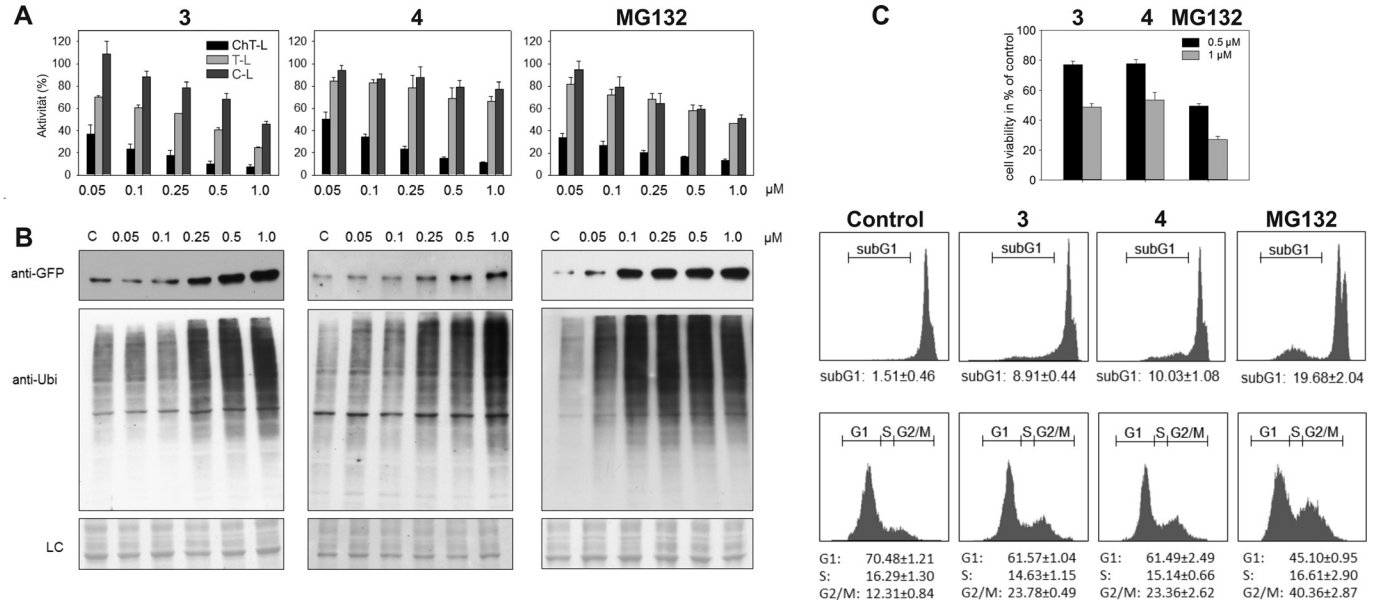

Figure 3. A) Inhibition of the ChT-L, T-L, and C-L activities by **3** and **4** compared to MG132 in HeLa cells. Relative activities are expressed as percentages normalized to a DMSO-treated control. B) Ubiquitin^{G76V}-GFP1 in ear fibroblasts of transgenic mice and ubiquitylated proteins markedly accumulate in the presence of increasing concentrations of **3**, **4**, and MG132 compared to DMSO alone. C) Staining was performed by western blot with anti-GFP and anti-ubiquitin (anti-Ubi) antibodies, respectively. Amido black staining of western blot membranes served as a control for equal protein loading (LC). C) The viability of HeLa cells exposed to **3**, **4**, or MG132 was assessed by a MTT assay. Cell cycle related changes (number of cells in G1, S and G2/M phases) and apoptotic cells (number of cells in sub-G1) were detected by flow cytometry analysis of the DNA content and normalized to a DMSO-treated control. For panels (A) and (C) values are given as the means of three independent experiments ± SEM.

diastereomers (2*R*, 3*S*)-**5** and (2*S*, 3*R*)-**5** did not inhibit the proteasome in HeLa cells and were inactive in the MTT assay (Figure S2). These results prove the robustness of the presented data and demonstrate that a single methyl group can be decisive not only for subunit selectivity but also for the entire biological activity of a compound.

In conclusion, we identified minimal structural elements that distinguish between β5c and β5i. Using the β-lactone scaffold as a streamlined proteasome inhibition motif, we synthesized two belactosin derivatives with valine- and isoleucine-like P1 side chains that exhibit exquisite potency in the low nanomolar range. We found that a single P1-methyl group creates a six-fold difference in potency for β5i. Selective inhibition can thus be achieved solely through the P1 site, a result of crucial importance for the future design of proteasome inhibitors. Furthermore, the reduced cytotoxicity compared to currently applied peptide proteasome inhibitors qualify these β-lactones as promising lead structures for applications in inflammatory diseases. In particular, derivatization of the dimethoxybenzyl side chain offers a great opportunity to extend these scaffolds towards the previously neglected primed substrate binding channel of β5c and β5i, as well as the other proteasomal active sites.

Keywords: cytotoxicity · immunoproteasome · inhibitors · lead structures · β-lactones

How to cite: *Angew. Chem. Int. Ed.* **2015**, *54*, 7810–7814
Angew. Chem. **2015**, *127*, 7921–7925

[1] E. M. Huber, M. Groll, *Angew. Chem. Int. Ed.* **2012**, *51*, 8708–8720; *Angew. Chem.* **2012**, *124*, 8838–8850.
[2] S. Murata, K. Sasaki, T. Kishimoto, S. Niwa, H. Hayashi, Y. Takahama, K. Tanaka, *Science* **2007**, *316*, 1349–1353.
[3] L. Borissenko, M. Groll, *Chem. Rev.* **2007**, *107*, 687–717.
[4] a) M. Groll, L. Ditzel, J. Löwe, D. Stock, M. Bochtler, H. D. Bartunik, R. Huber, *Nature* **1997**, *386*, 463–471; b) M. Orlowski, C. Cardozo, C. Michaud, *Biochemistry* **1993**, *32*, 1563–1572.
[5] a) M. Mishto, E. Bellavista, A. Santoro, A. Stolzing, C. Ligorio, B. Nacmias, L. Spazzafumo, M. Chiappelli, F. Licastro, S. Sorbi, A. Pession, T. Ohm, T. Grune, C. Franceschi, *Neurobiol. Aging* **2006**, *27*, 54–66; b) M. Diaz-Hernandez, F. Hernandez, E. Martin-Aparicio, P. Gomez-Ramos, M. A. Moran, J. G. Castano, I. Ferrer, J. Avila, J. J. Lucas, *J. Neurosci.* **2003**, *23*, 11653–11661.
[6] a) A. Visekruna, N. Slavova, S. Dullat, J. Grone, A. J. Kroesen, J. P. Ritz, H. J. Buhr, U. Steinhoff, *Int. J. Colorectal. Dis.* **2009**, *24*, 1133–1139; b) L. R. Fitzpatrick, V. Khare, J. S. Small, W. A. Koltun, *Dig. Dis. Sci.* **2006**, *51*, 1269–1276.
[7] Y. K. Ho, P. Bargagna-Mohan, M. Wehenkel, R. Mohan, K. B. Kim, *Chem. Biol.* **2007**, *14*, 419–430.
[8] a) T. Muchamuel, M. Basler, M. A. Aujay, E. Suzuki, K. W. Kalim, C. Lauer, C. Sylvain, E. R. Ring, J. Shields, J. Jiang, P. Shwonek, F. Parlati, S. D. Demo, M. K. Bennett, C. J. Kirk, M. Groettrup, *Nat. Med.* **2009**, *15*, 781–787; b) M. Basler, S. Mundt, T. Muchamuel, C. Moll, J. Jiang, M. Groettrup, C. J. Kirk, *EMBO Mol. Med.* **2014**, *6*, 226–238; c) H. T. Ichikawa, T. Conley, T. Muchamuel, J. Jiang, S. Lee, T. Owen, J. Barnard, S. Nevarez, B. I. Goldman, C. J. Kirk, R. J. Looney, J. H. Anolik, *Arthritis Rheum.* **2011**, *64*, 493–503.
[9] E. M. Huber, M. Basler, R. Schwab, W. Heinemeyer, C. J. Kirk, M. Groettrup, M. Groll, *Cell* **2012**, *148*, 727–738.
[10] G. de Bruin, E. M. Huber, B. T. Xin, E. J. van Rooden, K. Al-Ayed, K. B. Kim, A. F. Kisselev, C. Driessen, M. van der Stelt,

G. A. van der Marel, M. Groll, H. S. Overkleeft, *J. Med. Chem.* **2014**, *57*, 6197 – 6209.
[11] a) A. Asai, A. Hasegawa, K. Ochiai, Y. Yamashita, T. Mizukami, *J. Antibiot.* **2000**, *53*, 81 – 83; b) O. V. Larionov, A. de Meijere, *Org Lett.* **2004**, *6*, 2153 – 2156.
[12] a) G. Fenteany, R. F. Standaert, W. S. Lane, S. Choi, E. J. Corey, S. L. Schreiber, *Science* **1995**, *268*, 726 – 731; b) M. Groll, E. P. Balskus, E. N. Jacobsen, *J. Am. Chem. Soc.* **2008**, *130*, 14981 – 14983; c) A. List, E. Zeiler, N. Gallastegui, M. Rusch, C. Hedberg, S. A. Sieber, M. Groll, *Angew. Chem. Int. Ed.* **2014**, *53*, 571 – 574; *Angew. Chem.* **2014**, *126*, 582 – 585.
[13] M. Groll, O. V. Larionov, R. Huber, A. de Meijere, *Proc. Natl. Acad. Sci. USA* **2006**, *103*, 4576 – 4579.
[14] V. S. Korotkov, A. Ludwig, O. V. Larionov, A. V. Lygin, M. Groll, A. de Meijere, *Org. Biomol. Chem.* **2011**, *9*, 7791 – 7798.
[15] A. de Meijere, V. S. Korotkov, A. V. Lygin, O. V. Larionov, V. V. Sokolov, T. Graef, M. Es-Sayed, *Org. Biomol. Chem.* **2012**, *10*, 6363 – 6374.
[16] M. L. Stein, H. Cui, P. Beck, C. Dubiella, C. Voss, A. Kruger, B. Schmidt, M. Groll, *Angew. Chem. Int. Ed.* **2014**, *53*, 1679 – 1683; *Angew. Chem.* **2014**, *126*, 1705 – 1709.
[17] N. Gallastegui, M. Groll, *Methods Mol. Biol.* **2012**, *832*, 373 – 390.
[18] S. Kawamura, Y. Unno, A. List, A. Mizuno, M. Tanaka, T. Sasaki, M. Arisawa, A. Asai, M. Groll, S. Shuto, *J. Med. Chem.* **2013**, *56*, 3689 – 3700.
[19] a) M. Groll, B. C. Potts, *Curr. Top. Med. Chem.* **2011**, *11*, 2850 – 2878; b) M. Groll, R. Huber, B. C. Potts, *J. Am. Chem. Soc.* **2006**, *128*, 5136 – 5141.

Received: March 30, 2015
Published online: May 14, 2015

